Journal of Engineering and Applied Sciences 13 (1): 157-161, 2018
ISSN: 1816-949X

Study on the Characteristic of Air Flow of Shark Antennas for Each of the Configurations by using Simulated Flow Analysis

[1]Kye-Kwang Choi and [2]Jae-Ung Cho
[1]Department of Metal Mold Design Engineering,
[2]Division of Mechanical and Automotive Engineering, Kongju National University,
1223-24 Cheonan Daero, Seobuk-gu, 31080 Cheonan-si, Chungnam, Korea

Abstract: With the knowledge that the air resistance acting on the body of automobile when it is driven at high velocity is directly related to the fuel efficiency, it is now being considered as a highly important issue in designing of automobile. This study aims to research how the velocity, pressure and phenomenon of turbulence due to the air flow occurring around the shark antenna of automobile are generated when the vehicle is running and what effects they have. In this study, commercially available shark antenna models are 3D modeled with CATIVA design program and the simulated flow analysis was executed on these models by using ANSYS finite-element analysis program. After having 3D designed the shark antenna models for each of the configurations, it was possible to confirm the characteristics of the air flow of each of the shark antenna models by executing flow analysis. As the results of the research, it was determined that the K-type shark antenna model is the most appropriate model for application to vehicles since it displayed lower values in all the comparison items including maximum flux, maximum pressure and distribution area of high pressure in comparison to those of the H-type and G-type shark antenna model. Accordingly, it is deemed that this model can make contributions towards the reduction in the resistance against air and the ensuring improvement of fuel efficiency, etc. This study is on the research of the air flow of shark antenna applied to automobiles. It is deemed that the data secured through the corresponding research can be used as basic data for more advanced shark antenna design and researches related to the characteristics of air flow of automobile being driven.

Key words: Shark antenna, configuration, velocity, pressure, characteristic, flow analysis

INTRODUCTION

With the knowledge that the air resistance acting on the body of automobile when it is driven at high velocity is directly related to the fuel efficiency, it is now being considered as a highly important issue in designing of automobile (Rotaru, 2017; Sourdis, 2015). However, it is somewhat difficult to apply the air dynamics applied to airplanes to the automobile because the characteristic of flow field formed around automobile is substantially different from that of the airplane. In particular, due to the characteristics of the automobile that places high value to the external beauty of the vehicle, it is not possible to reflect only the aerodynamic factors onto the design at the time of the designing of the exterior of the vehicle (Shaidarova *et al*., 2017; Han *et al*., 2017; Eckhardt, 2017; Creamers, 2017). Accordingly, the configurations that appropriately consider the design aspect of the vehicle are designed. The diversified and complex phenomenon is generated as the air flows around the vehicle when it runs at high velocity (Kim *et al*., 2017; Manimaran and Senthilkumar, 2016). Moreover, appropriate controlling of the occurrence of such turbulence phenomenon is an important issue in improving the aerodynamic performance of the automobile. Accordingly, this study aims to research how the velocity, the pressure and phenomenon of turbulence due to the air flow occurring around the shark antenna of automobile are generated when the vehicle is running and what effects they have by focusing on these issues (Salehifar *et al*., 2016; Ren *et al*., 2016).

MATERIALS AND METHODS

In this study, commercially available shark antenna models are 3D modeled with CATIVA design program

Corresponding Author: Jae-Ung Cho, Division of Mechanical and Automotive Engineering, Kongju National University, 1223-24 Cheonan Daero, Seobuk-gu, 31080 Cheonan-si, Chungnam, Korea

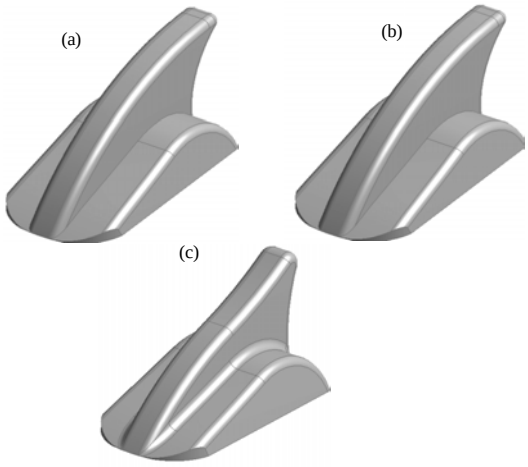

Fig. 1: Research models: a) H-type Model; b) K-type Model and c) G-type Model

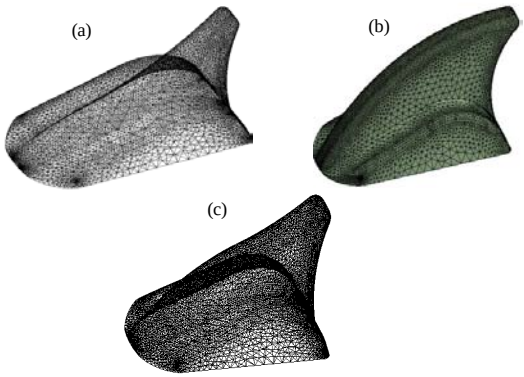

Fig. 2: Mesh conditions of research models: a) H-type Model; b) K-type Model and c) G-type Model

Table 1: Material properties

Materials	Stainless steel
Density (kg/m^3)	7750.00
Young's Modulus (GPa)	193.00
Poisson's ratio	0.31
Yield strength (MPa)	207.00
Ultimate strength (MPa)	586.00

and the simulated flow analysis was executed on these models. Figure 1 illustrates the appearances of various shark antenna models and all the shark antenna models have the same dimensions of length of 1400 mm, width of 700 mm and height of 700 mm. Table 1 lists the material properties of the shark antenna models (Zhou *et al*., 2016; Sampaio and Garcia, 2016; Ervin *et al*., 2016; Sunderland *et al*., 2016).

Boundary conditions: Figure 2 illustrates the Mesh conditions applied to each of the shark antenna models to carry out simulated flow analysis while Fig. 3 illustrates

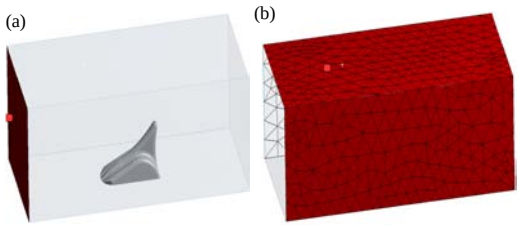

Fig. 3: Boundary conditions of research models: a) Inlet and b) Opening

the boundary conditions applied to the shark antenna models. The boundary conditions applied to the specimen models are the same and the velocity of the air flux as the vehicle velocity of 100 km/h was set by applying Inlet conditions to the model first in order to observe the air flow that occurs at the time of the running of the vehicle. Opening conditions of the temperature of 25°C and 1 atmospheric pressure were applied to the both lateral sides, top and rear of the models. In addition, the road condition was applied by presuming that the bottom of the model is attached to the outer ceiling of the automobile.

RESULTS AND DISCUSSION

Figure 4 illustrates the resultant values of flux generated in the H-type shark antenna model among the flow analysis of each of the shark antenna models. As the results of the execution of analysis, the flux generated at the H-type shark antenna model during running displayed the tendency of gradual increase in the front portion and the process of the flow of the air going over from the front to the back of the corresponding model. At this time the maximum flux was found to be approximately 144.9 m/sec. After having reached the maximum flux, it rapidly drops to the minimum flux of approximately 0.68 m/sec at the back of the shark antenna model.

Figure 5 illustrates the resultant values of flux generated in the K-type shark antenna model among the flow analysis of each of the shark antenna models. As the results of the execution of analysis, trends similar to the aforementioned H-type shark antenna model were displayed. The flux generated at the K-type shark antenna model during running displayed the tendency of gradual increase in the front portion and the process of the flow of the air going over from the front to the back of the corresponding model. At this time, the maximum flux was found to be approximately 36.42 m/sec. After having reached the maximum flux, it rapidly drops to the minimum flux of approximately 0.28 m/sec at the back of the shark antenna model.

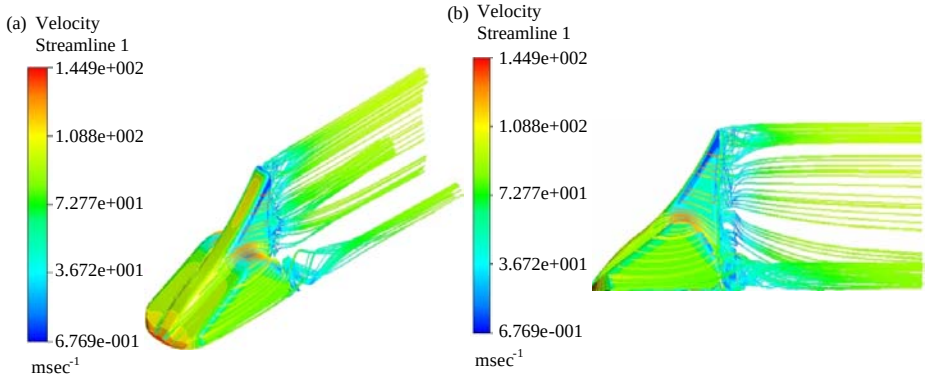

Fig. 4: Velocity results of H-type shark antenna model

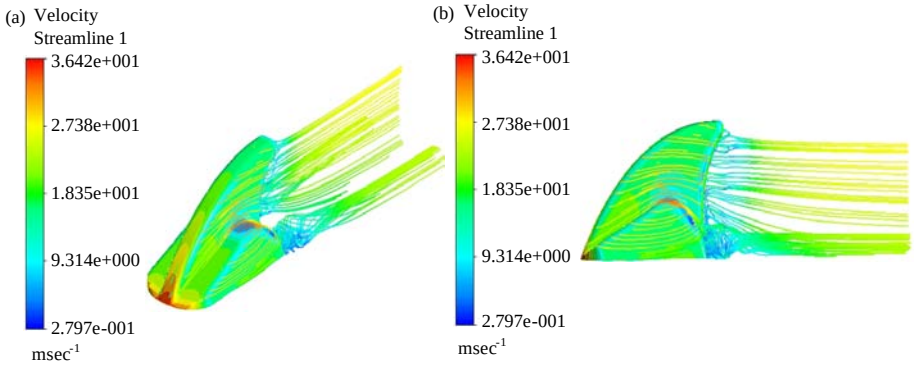

Fig. 5: Velocity results of K-type shark antenna model

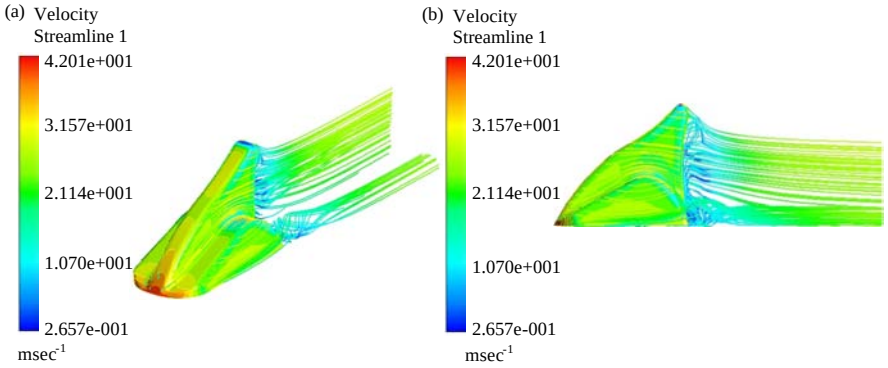

Fig. 6: Velocity results of G-type shark antenna model

Figure 6 illustrates the resultant values of flux generated in the G-type shark antenna model. As the results of the execution of analysis, the trends similar to the aforementioned H-type and K-type shark antenna models were displayed. The flux generated at the G-type shark antenna model during running displayed the tendency of gradual increase in the front portion and the process of the flow of the air going over from the front to the back of the corresponding model. At this time, the maximum flux was found to be approximately 42.01 m/sec. After having reached the maximum flux, it rapidly drops to the minimum flux of approximately 0.266 m/sec at the back of the shark antenna model.

Figure 7 illustrates the pressure exerted onto the shark antenna model by the flow of air while the vehicle is running. Firstly, as the results of the analysis of the H-type shark antenna model, the maximum pressure was observed at the foremost front portion of the

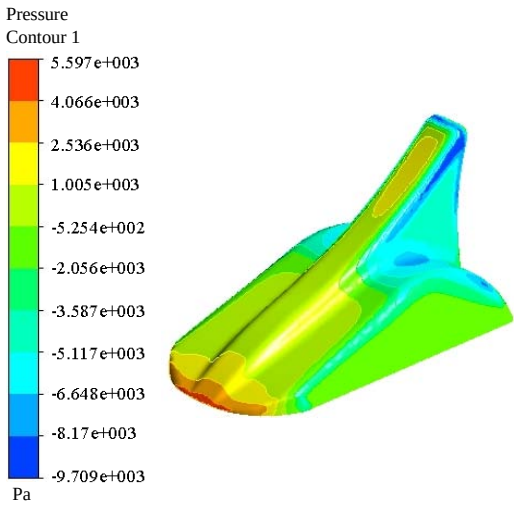

Fig. 7: Pressure result of H-type shark antenna model

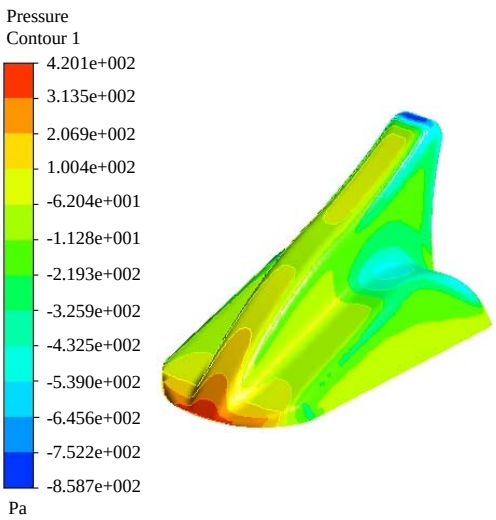

Fig. 9: Pressure result of G-type shark antenna model

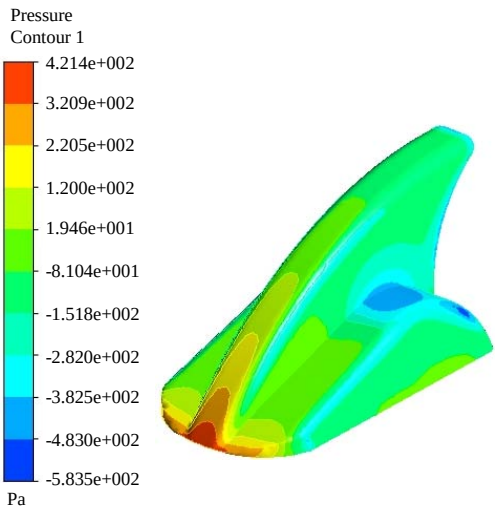

Fig. 8: Pressure result of K-type shark antenna model

corresponding model and the pressure displayed the tendency of gradual decrease towards the rear potion of the shark antenna model in accordance with such flow of the air. At this time, the maximum pressure generated at the H-type shark antenna model was found to be approximately 0.00560 MPa.

Figure 8 illustrates the pressure generated at the K-type shark antenna model in accordance with the flow of the air while the vehicle is running. Similar to the H-type shark antenna model, the maximum pressure was observed at the foremost front portion of the corresponding model and the pressure displayed the tendency of gradual decrease towards the rear potion of the shark antenna model. At this time, the maximum pressure generated at the K-type shark antenna model was found to be approximately 0.0004214 MPa. Unlike the K-type shark antenna model, there were smaller areas of the antenna that displayed high pressures.

Table 2: Comparison analysis results of models

Models	Maximum velocity (m/sec)	Maximum pressure (MPa)
H-type shark antenna	144.90	0.0056000
K-type shark antenna	36.42	0.0004214
G-type shark antenna	42.01	0.0004201

Figure 9 illustrates the pressure generated at the G-type shark antenna model in accordance with the flow of the air while the vehicle is running. It displayed tendency that is similar to those of the H-type and K-type shark antenna models. Accordingly, the maximum pressure was observed at the foremost front portion of the corresponding model and the pressure displayed the tendency of gradual decrease towards the rear potion of the shark antenna model. At this time, the maximum pressure generated at the K-type shark antenna model was found to be approximately 0.0004201 MPa.

Comparison of analysis results and considerations: Table 2 mutually compares the resultant values of the flow analysis on each of the shark antenna models. When three shark antenna models are mutually compared, the maximum flux of H-type shark antenna model was approximately 144.9 m/sec with the maximum pressure of approximately 0.00560 Mpa while the maximum flux of K-type shark antenna model was approximately 36.42 m/sec with the maximum pressure of approximately 0.0004214 Mpa. In the case of G-type shark antenna model, the maximum flux was found to be approximately 42.01 m/sec with the maximum pressure of approximately

0.0004201 MPa. As the results of the research, K-type shark antenna model was determined to be the model most appropriate for application to vehicles as it had lower values in all the comparison items including maximum flux, maximum pressure and distribution area of high pressure in comparison to both the H-type and G-type shark antenna models. As such, it is deemed to be a model that can make contributions towards the reduction in resistance against air and improvement in the fuel efficiency, etc.

CONCLUSION

In this study, the following conclusions were derived by executing simulated flow analysis on a total of three shark antenna models, namely, H-type, K-type and G-type shark antenna model. It was possible to confirm the characteristics of air flow of each of the shark antenna models by executing flow analysis after having 3D designed the said models for each of the configurations.

When three shark antenna models for each of the configurations are mutually compared, the maximum flux of H-type shark antenna model was approximately 144.9 m/sec with the maximum pressure of approximately 0.00560 MPa while the maximum flux of K-type shark antenna model was approximately 36.42 m/sec with the maximum pressure of approximately 0.0004214 MPa. In the case of G-type shark antenna model, the maximum flux was found to be approximately 42.01 m/sec with the maximum pressure of approximately 0.0004201 MPa.

As the results of the research, K-type shark antenna model was determined to be the model most appropriate for application to vehicles as it had lower values in all the comparison items including maximum flux, maximum pressure and distribution area of high pressure in comparison to both the H-type shark antenna model and the G-type shark antenna model. As such, it is deemed to be a model that can make contributions towards the reduction in resistance against air and improvement in the fuel efficiency, etc.

This study is on the research of the air flow of shark antenna applied to automobiles. It is deemed that the data secured through the corresponding research can be used as basic data for more advanced shark antenna design and researches related to the characteristics of air flow of automobile being driven.

REFERENCES

Creamers, E.M.P., 2017. Implementation of erythroid lineage analysis by flow cytometry in diagnostic models for myelodysplastic syndromes. Haematologica, 102: 320-326.

Eckhardt, J., 2017. The inverse spectral transform for the conservative Camassa-Holm flow with decaying initial data. Arch. Ration. Mech. Anal., 224: 21-52.

Ervin, V.J., H. Lee and A.J. Salgado, 2016. Generalized Newtonian fluid flow through a porous medium. J. Math. Anal. Appl., 433: 603-621.

Han, D., A. Brylev, X. Yang and Z. Tan, 2017. Numerical analysis of second order, fully discrete energy stable schemes for phase field models of two-phase incompressible flows. J. Sci. Comput., 70: 965-989.

Kim, M., S.M. Lee, D.W. Lee, S. Park and S. Kim, 2017. Tribological effects of a rough surface bearing using an average flow analysis with a contact model of asperities. Intl. J. Precis. Eng. Manuf., 18: 99-107.

Manimaran, R. and R. Senthilkumar, 2016. Performance analysis of solar water heater at possible flow rates with and without phase change material. Distrib. Gener. Altern. Energy J., 31: 67-80.

Ren, Z., W. Li, R. Billinton and W. Yan, 2016. Probabilistic power flow analysis based on the stochastic response surface method. IEEE. Trans. Power Syst., 31: 2307-2315.

Rotaru, A., 2017. Thermal and kinetic study of hexagonal boric acid versus triclinic boric acid in air flow. J. Therm. Anal. Calorim., 127: 755-763.

Salehifar, M., M. Tahani, M. Hojaji and A. Dartoomian, 2016. CFD modeling for flow field characterization and performance analysis of HGITVC. Appl. Therm. Eng., 103: 291-304.

Sampaio, L. and A. Garcia, 2016. Exploring context-sensitive data flow analysis for early vulnerability detection. J. Syst. Software, 113: 337-361.

Shaidarova, L.G., I.A. Chelnokova, M.A. Il'ina, A.V. Gedmina and H.C. Budnikov, 2017. Amperometric detection of hydroxypurines at an electrode modified with a composite based on mixed-valence ruthenium and cobalt oxides in flow injection analysis. J. Anal. Chem., 72: 107-112.

Sourdis, C., 2015. Analysis of an irregular boundary layer behavior for the steady state flow of a Boussinesq fluid. Discrete Continuous Dyn. Syst., 37: 1039-1060.

Sunderland, K., M. Coppo, M. Conlon and R. Turri, 2016. A correction current injection method for power flow analysis of unbalanced multiple-grounded 4-wire distribution networks. Electric. Power Syst. Res., 132: 30-38.

Zhou, X., Y. Hu and J. Wang, 2016. Experimental analysis on flow past circular cylinder attached to frontal splitter plate. J. Beijing Univ. Aeronaut. Astronautics, 42: 172-179.